SPACE CHARGE MITIGATION WITH LONGITUDINALLY HOLLOW BUNCHES

A. Oeftiger*, S. Hancock, G. Rumolo, CERN, Meyrin, Switzerland

Abstract

Hollow longitudinal phase space distributions have a flat profile and hence reduce the impact of transverse space charge. Dipolar parametric excitation with the phase loop feedback systems provides such hollow distributions under reproducible conditions. We present a procedure to create hollow bunches during the acceleration ramp of CERN's PS Booster machine with minimal changes to the operational cycle. The improvements during the injection plateau of the downstream Proton Synchrotron are assessed in comparison to standard parabolic bunches.

INTRODUCTION

In the framework of the LHC Injectors Upgrade (LIU) project, the Large Hadron Collider (LHC) will have to be provided with beams of double intensity N but approximately the same transverse normalised emittances $\epsilon_{x,y}$ compared to present operation [1]. Each synchrotron of the LHC injector chain has been assigned an emittance blow-up and beam loss budget [2, Table 1]. In particular, the Proton Synchrotron (PS) is allowed a budget of $\Delta\epsilon/\epsilon_{\text{ini}} \leq 5\%$ and $\Delta N/N_{\text{ini}} \leq 5\%$. For the LIU beam parameters, the present pre-LIU machine conditions are found to exceed these values [3] which is why a series of machine upgrades are foreseen [4].

The most important limiting factor in the PS is direct space charge. Since the incoherent transverse space charge tune spread scales with the inverse energy,the 1.2 s long PS injection plateau during the standard double-batch (72-bunches) 25 ns LHC beam production is the most critical time. Therefore, the injection energy will be increased from the present $E_{\text{kin}} = 1.4\,\text{GeV}$ to 2 GeV.

Given the constraints on the normalised transverse emittances, intensity and bunch length, a further common strategy to mitigate space charge impact is to reshape the longitudinal beam profile of the usually Gaussian or even rather quasi-parabolic bunches. The canonical approach is to use a double RF harmonic in bunch lengthening mode (BLM) during the critical cycle times to diminish (or cancel) phase focusing around the RF bucket centre. This RF potential deformation results in both a larger RF bucket area (longitudinal acceptance) and flatter iso-Hamiltonian contours around the centre (and therefore bunch distributions with depressed line densities). An alternative to reshaping the longitudinal profile indirectly via a modified Hamiltonian is to alter the phase space distribution directly. This consideration leads us to the concept of "hollow" bunches. Figure 1 illustrates these two cases by plotting the longitudinal phase space (z, δ) with z the longitudinal bucket centre offset, $\delta = (p - p_0)/p_0$ the relative momentum deviation and p_0 the total momentum.

* adrian.oeftiger@cern.ch, also at EPFL, Lausanne, Switzerland

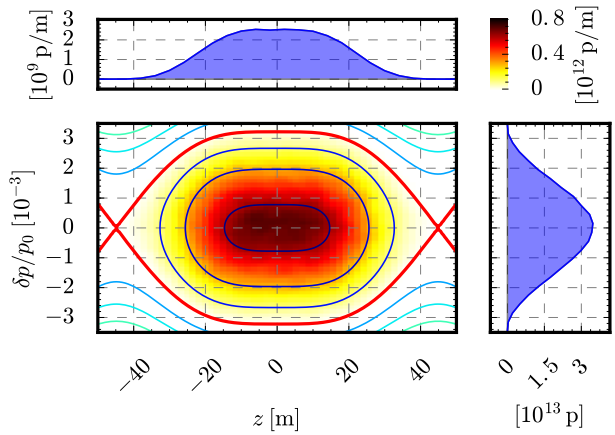

(a) Double-harmonic bucket in BLM (i.e. 180° relative phase and $V_{h=2} = V_{h=1}/2$) populated with a matched distribution (note the quasi-Gaussian distribution in the momentum projection).

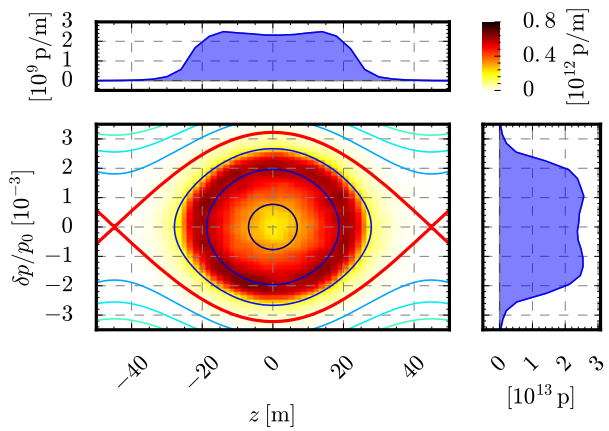

(b) Single-harmonic bucket at the same fundamental RF voltage populated with a hollow distribution. The spatial projection is flat equivalent to the second harmonic case, but additionally also the momentum projection becomes flat.

Figure 1: Longitudinal phase space plots (z, δ) from PyHEADTAIL simulations comparing between double-harmonic shaped and hollow bunches.

The lower left shows the momentum δ versus the coordinate z, the separatrix in red encloses the RF bucket. The density of the particle distribution is given by the heat map in the upper right corner. In addition, the iso-Hamiltonian contours indicate the momentary flow of particle trajectories. The upper plot shows the spatial projection and the plot to the right the momentum projection.

In this paper, we present hollow bunches as a viable additional tool to mitigate space charge and hence to reach the required LIU goals. This study has been tailored to the characteristics of LHC beams and involves minimal changes

ISBN 978-3-95450-178-6

to the currently PSB operational cycles. Nevertheless, the general applicability and potential of the concept become apparent. The idea is to create hollow bunches in the Proton Synchrotron Booster (PSB) and subsequently transfer them to the PS to overcome the brightness limits given by the affordable emittance blow-up during the PS injection plateau.

The structure of the following sections is laid out as follows: at first, we discuss the theoretical reasoning behind the idea. Then, we describe the procedure to reliably create hollow longitudinal distributions during the PSB acceleration ramp. Thirdly, the approach to extract the transverse emittances from the inherently non-Gaussian horizontal beam profiles (due to dispersion) is explained. Finally, we present the improvements measured for the hollow beams in comparison to the standard LHC-type beams. This paper is meant to complement and elaborate on our previously reported findings in [5]. Our efforts build on the experience from past hollow bunch experiments [6, 7].

THEORETICAL CONSIDERATIONS

For a transversely Gaussian normal distributed bunch of particles in a circular accelerator, the detuning effect of the beam self-fields can be quantified in terms of the transverse space charge tune spread [8],

$$\Delta Q_u(z) = -\frac{r_p \lambda(z)}{2\pi\beta^2\gamma^3} \oint ds \frac{\beta_u(s)}{\sigma_u(s)\left(\sigma_x(s)+\sigma_y(s)\right)} \quad (1)$$

with $u = x$ or $u = y$ for the horizontal resp. vertical plane, z denoting the longitudinal position with respect to the beam centre-of-gravity, $\lambda(z)$ the line charge density in C/m, r_p the classic particle radius, β the speed in units of speed of light, γ the Lorentz factor, $\beta_u(s)$ the betatron function depending on the longitudinal location s around the accelerator ring and $\sigma_u(s)$ the corresponding transverse beam sizes. In presence of dispersion $D_x(s)$, the momentum distribution contributes to the horizontal beam size. Assuming also the momentum distribution to be Gaussian normal distributed yields the well-known expression

$$\sigma_x(s) = \sqrt{\frac{\beta_x(s)\epsilon_x}{\beta\gamma} + D_x^2(s)\delta_{\text{rms}}^2} \quad , \quad (2)$$

where ϵ_x is the normalised beam emittance and δ_{rms} the root mean square of the relative momentum distribution. NB: Eq. (2) is no longer valid for beams with a momentum distribution that significantly deviates from a Gaussian.

From Eq. (1) it immediately follows that

1. space charge scales with the inverse energy, $\Delta Q_u \propto 1/(\beta\gamma^2)$, hence the most critical cycle time for an accelerator is around the injection;
2. reducing the peak line density λ_{max} decreases the maximum tune shift; and
3. a broader momentum distribution leads to larger horizontal beam sizes and hence a smaller tune spread (cf. Eq. (2) when increasing δ_{rms}).

Reducing the incoherent tune spread makes the beam less prone to betatron resonances located near the working point [9] – such as the integer resonance which causes the observed critical emittance growth in the PS [3].

Longitudinally hollow phase space distributions address the latter two aspects of Eq. (1) to reduce ΔQ_u^{max} compared to Gaussian or parabolic bunches. Figure 1b exhibits the intrinsically flattened $\lambda(z)$ as well as the increased δ_{rms}. The increased momentum spread is an evident advantage of hollow distributions over double-harmonics, which becomes apparent comparing the momentum projections between Fig. 1b and Fig. 1a.

HOW TO CREATE HOLLOW BUNCHES

Dipolar Parametric Resonances

The mechanism we exploit to create hollow bunches is based on driving a longitudinal parametric resonance by phase modulation [10]. To this end, we use the PSB phase loop system which aligns the RF reference phase ϕ_{rf} with the centre-of-gravity of the bunch. By modulating ϕ_{rf} around the synchronous phase ϕ_S,

$$\phi_{\text{rf}}(t) = \phi_S + \hat{\phi}_{\text{drive}} \sin(\omega_{\text{drive}} t) \quad , \quad (3)$$

we excite the dipole mode of the resonance. For this, the driving frequency ω_{drive} needs to satisfy the resonance condition

$$m\,\omega_{\text{drive}} \simeq n\,\omega_S \quad , \quad (4)$$

where ω_S denotes the angular synchrotron frequency. The integer numbers m and n characterise the m:n parametric resonance. The $m = n = 1$ resonance proves most useful for our purposes – higher harmonic resonances deplete the bunch centre less as they produce two or more filaments pointing outwards from the core (instead of just one). Figure 2 depicts such a measured phase space $(\phi, \Delta E)$ distribution (with $\phi = -hz/R$ and $\Delta E = \delta p_0 c/\beta$ for h the harmonic and R the radius) resulting from driving the 1:2 resonance.

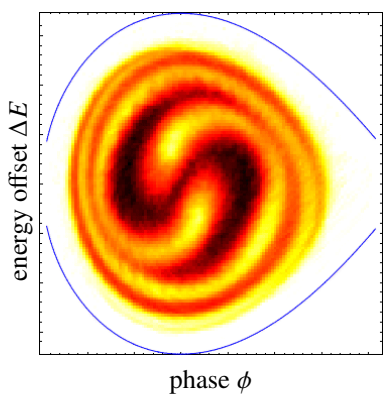

Figure 2: Longitudinal phase space $(\phi, \Delta E)$ for the 1:2 resonance via phase space tomography [11] in the PSB.

ISBN 978-3-95450-178-6

Two main factors suppress the linear synchrotron frequency [12, Eq. (3.16)]

$$\omega_{S,0} = \omega_{\mathrm{rev}} \sqrt{\frac{hqV_{\mathrm{RF}}|\eta\cos(\phi_S)|}{2\pi p_0 \beta c}} \quad , \tag{5}$$

where q denotes the particle charge, V_{RF} the RF voltage, $\eta \doteq \gamma_{\mathrm{tr}}^{-2} - \gamma^{-2}$ the slippage factor (with γ_{tr} the transition energy), and ω_{rev} the angular revolution frequency. The *RF bucket non-linearities* decrease the synchrotron tune for non-zero synchrotron amplitudes $\tilde{\phi}$ towards the separatrix by [12, Eq. (3.60)]

$$\omega_{S,\mathrm{nl}}(\tilde{\phi}) = \frac{\pi\omega_{S,0}}{2K(\sin(\tilde{\phi}/2))} \approx \left(1 - \frac{\tilde{\phi}^2}{16}\right)\omega_{S,0} \tag{6}$$

with $K(k)$ the complete elliptic integral of the first kind. Furthermore, since the PSB operates below transition, $\eta < 0$, *longitudinal space charge* additionally reduces ω_S. The linearised expression for a matched Gaussian-type bunch reads [13, Eq. (1.47)]

$$\omega_S^2(N,\tilde{\phi}) = \omega_{S,\mathrm{nl}}^2(\tilde{\phi}) + \frac{\omega_{\mathrm{rev}}^2}{\sqrt{2\pi}\sigma_z^3}\frac{Nr_p\eta R^2 g}{\beta^2\gamma^3} \quad , \tag{7}$$

with g the geometry factor taking into account the bunch aspect ratio as well as indirect space charge from a perfectly conducting vacuum tube [14].

PyHEADTAIL Simulations

We have carried out extensive studies of the bunch modulation with the collective effects simulation software PyHEADTAIL [15, 16]. Longitudinal space charge has been included via a line density derivative model [17]. By driving the 1:1 resonance at a frequency slightly below the linear synchrotron frequency, $\omega_{\mathrm{drive}} \approx 0.9\omega_{S,\mathrm{lin}}$ (accounting for the aforementioned detuning effects), the particles in the bunch core are excited to higher synchrotron amplitudes. Figure 3 shows the depletion process of the bunch centre within a few synchrotron periods during the acceleration ramp leading to hollow longitudinal phase space distributions. In this particular case, the Gaussian distributed bunch started from a longitudinal r.m.s. emittance of $\epsilon_z = 1.12\,\mathrm{eV\,s}$ at $E_{\mathrm{kin}} = 0.7\,\mathrm{GeV}$. The resonance has been excited at $\hat{\phi}_{\mathrm{drive}} = 18°$ for a frequency of $\omega_{\mathrm{drive}}/(2\pi) = 760\,\mathrm{Hz}$ during $T_S = 6$ synchrotron periods. We have used 512 fixed slices across the bucket and 2×10^6 macro-particles to fully resolve the dynamically changing space charge potential of the oscillating bunch.

The synchrotron frequency spread due to Eq. (6) between the inner- and outer-most particles leads to a filamentation-like angular spread. The modulation duration determines the azimuthal span to which the excited particles surround the depleted bucket centre. The optimal duration distributing the particles as evenly as possible depends in descending importance on the excitation amplitude $\hat{\phi}_{\mathrm{drive}}$, the ratio between longitudinal emittance ϵ_z and bucket acceptance, and finally the beam intensity. The latter dependency becomes apparent during intensity scans up until $N = 6.4\times10^{12}$, where we find the obtained depletion of the resulting phase space distribution to decrease with increasing N [18].

As laid out before, Eq. (7) predicts an additional detuning from space charge. To compare this with the effect from the bucket non-linearities, Eq. (6), we ran longitudinal simulations during $T_S = 100$ in the PSB ($\eta < 0$) for various intensities. All simulation runs start from the same initial Gaussian distribution with $\sigma_z = 15\,\mathrm{m}$ r.m.s. bunch length. We fix particles at synchrotron amplitudes across the whole bunch and extract their synchrotron tune by Fourier transforming their synchrotron motion. These values are plotted in Figure 4 versus the respective initial synchrotron amplitudes, which are expressed as the maximal spatial amplitude z_{max} of the particle's trajectory.

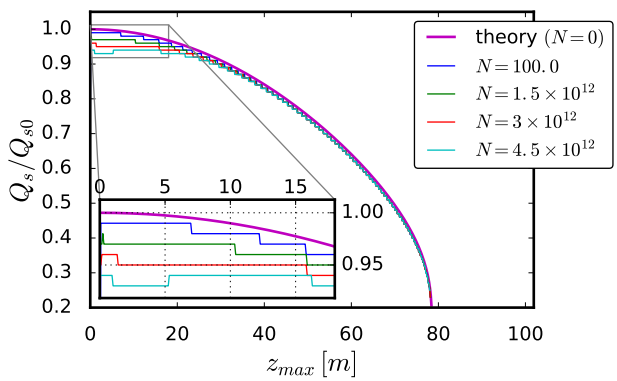

Figure 4: Normalised actual synchrotron frequency $Q_S/Q_{S,0} \equiv \omega_S/\omega_{S,0}$ vs. synchrotron amplitude expressed in $z_{\mathrm{max}} = \tilde{\phi}R/h$, the violet line corresponds to Eq. (6).

At $z_{max} = 0$ one can directly observe the tune depression given by Eq. (7). Then, for larger synchrotron amplitudes to-

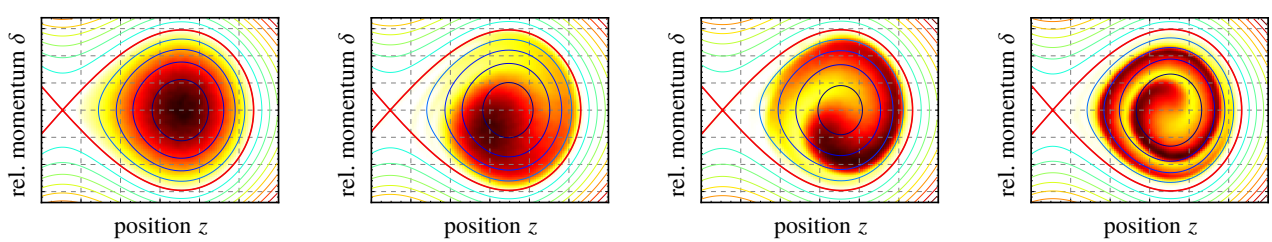

(a) PSB C575, Gaussian start. (b) PSB C579, after $3.5T_S$. (c) PSB C583, after $6T_S$. (d) PSB C591, filamenting.

Figure 3: Longitudinal phase space (z, δ) during the PyHEADTAIL simulation illustrating the dipolar parametric resonance.

ISBN 978-3-95450-178-6

wards the bucket separatrix, the non-linear sinusoidal bucket additionally reduces the linearised synchrotron tune.

Without space charge for $N = 0$, one obtains a certain tune spread across the bunch comparing the bucket centre $z_{max} = 0$ to the bunch ends at $z_{max} = 2\sigma_z = 30\,\mathrm{m}$. This effect becomes even more pronounced if one would move the bunch centre to non-zero z (which is the case for the parametric resonance). The closer we shift the bunch centre towards the separatrix, the larger the synchrotron tune spreads across the bunch. This is precisely the mechanism that leads to the angular spreading of the bunch in longitudinal phase space during the parametric resonance depletion procedure.

Now, adding the space charge effect, Fig. 4 reveals that at larger intensities N the tune spread across the bunch diminishes (compare again between $z_{max} = 0$ and $z_{max} = 30\,\mathrm{m}$). For $N = 4.5 \times 10^{12}$, the Gaussian bunch imprints a nearly constant plateau onto the nearly parabolically decreasing $N = 0$ synchrotron tune curve: space charge makes the bunch resist phase focusing. (At yet larger intensities or smaller σ_z the tune around the origin would even turn into a local dip.) This effect is known as suppression of decoherence by space charge [19].

The analysis in terms of frequency spread also provides a possible remedy: the absolute tune spread ΔQ_S per Δz due to the bucket non-linearities (i.e. the derivative of the magenta curve in Figure 4) evidently increases towards the separatrix. Therefore, exciting the particles to higher synchrotron amplitudes by means of a larger driving amplitude $\hat{\phi}_{\mathrm{drive}}$ may restore a sufficient synchrotron tune spread across the bunch in order to surround the bucket centre with particles.

To sum up, the final longitudinal emittance ϵ_z varies with the bunch intensity, modulation duration and amplitude. In order to reach a specific ϵ_z, modifying $\hat{\phi}_{\mathrm{drive}}$ turns out to be the most effective parameter, while the excitation duration is fixed beforehand by maximising the azimuthal phase space distribution.

Implementation in PSB

As reported in [5], based on the current operational LHC-type beam set-up, we introduced the phase modulation at cycle time C575 (corresponding to an intermediate energy of $E_{\mathrm{kin}} = 0.71\,\mathrm{GeV}$) in a single harmonic accelerating bucket. During 9 ms equivalent to 6 synchrotron periods the beam is driven onto the resonance starting from an initial matched longitudinal emittance of $\epsilon_{z,100\%} \approx 1.1\,\mathrm{eV\,s}$. With these settings, the resulting distributions appeared consistently and reproducibly depleted.

Varying the driving frequency for the parametric resonance revealed a broad resonance window. The beam turned out to be correctly excited for frequencies in the range

$$649\,\mathrm{Hz} \leq \frac{\omega_{\mathrm{drive}}}{2\pi} \leq 734\,\mathrm{Hz} \quad . \tag{8}$$

This resonance window is sharply defined up to 1 Hz.

Special attention had to be given to optimise the phase loop gain during the excitation process: for a too strong gain, the phase loop continuously realigns the phase of the main C02 cavities with the beam. This counteracts the excitation and leads to severely perturbed distributions. Our first experiment series using the radial loop instead of the phase loop for the phase modulation was in fact severely affected by this phase loop action [20].

Eventually, the long filament can be smoothed to a ring-like phase space distribution by high frequency phase modulation at harmonic $h = 9$ with the C16 cavities. Figure 5 shows tomographic reconstructions [11] of longitudinal phase space at important cycle times. The horizontal axis is reverted compared to Fig. 3, since $\phi = -hz/R$. Note the coincidence of the phase space distributions at cycle time C591 between simulation results in Fig. 3d and measurement in Fig. 5b.

SPACE CHARGE MITIGATION IN PS

To assess the impact of direct space charge during the 1.2 s PS injection plateau at $E_{\mathrm{kin}} = 1.4\,\mathrm{GeV}$ and $h = 7$, we compare single bunch beams of the usual LHC parabolic type with the modified hollow type by measuring transverse emittance blow-up and beam loss. For each shot, tomography and wire scans yield the z, δ, x, y distributions 15 ms after injection and again 20 ms before the second batch injection time. Table 1 lists the experiment parameters.

Emittance Determination with Dispersion Effects

Hollow bunches exhibit a non-Gaussian δ distribution by construction, therefore Eq. (2) does not apply. In principle,

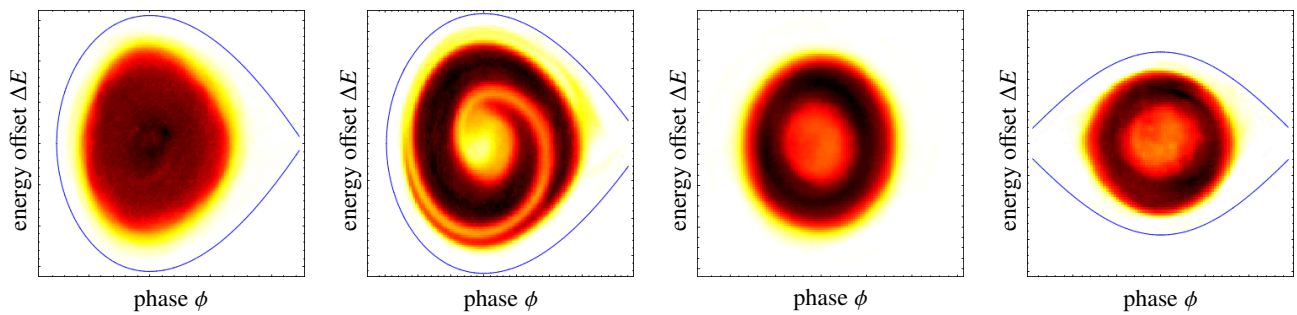

(a) PSB C573, before excitation. (b) PSB C591, after excitation. (c) PSB C800 (5 ms to extract.). (d) PS C171 (1 ms after inject.).

Figure 5: Longitudinal phase space $(\phi, \Delta E)$ reconstructed via tomography at different stages in the PSB (measurements) [5].

ISBN 978-3-95450-178-6

Table 1: Relevant Experiment Beam Parameters for PS

parameter	hollow value	parabolic value
N	$(1.66 \pm 0.05) \times 10^{12}$	$(1.84 \pm 0.03) \times 10^{12}$
$\epsilon_{z,100\%}$	1.43 ± 0.15 eV s	1.47 ± 0.11 eV s
$\epsilon_{z,\mathrm{rms}}$	0.32 ± 0.02 eV s	0.3 ± 0.01 eV s
Q_x, Q_y	(6.23, 6.22)	

each particle's horizontal position is a sum of two independent random variables, the f_β-distributed betatron motion x_β and the f_{disp}-distributed dispersion contribution $D_x\delta$,

$$x = x_\beta + D_x\delta \quad , \tag{9}$$

where $D_x = 2.3$ m at the wire scanner. Therefore, the horizontal distribution function is given by the convolution

$$p(x) = \int dx'\, f_\beta(x') f_{\mathrm{disp}}(x - x') \tag{10}$$

$$\text{with} \quad f_{\mathrm{disp}}(x) = f_\delta(D_x\delta)/|D_x| \quad . \tag{11}$$

Considering the beam as an ensemble, we have measured f_{disp} (via tomography) as well as p (the wire scanner profile). Assuming f_β to be Gaussian distributed, we can determine its variance σ_β^2 and hence the normalised emittance

$$\epsilon_x = \beta\gamma\sigma_\beta^2/\beta_x \tag{12}$$

via a least squares algorithm by comparing the convolution of the educated guess for f_β and the measured f_{disp} with the measured p, cf. Fig. 6. Applying this procedure to both beams, we find Eq. (2) to underestimate ϵ_x from 24.8% to 34.8% for both the parabolic as well as the hollow bunches.

Experimental Results

As discussed in [5], we prepare both beam types with varying bunch lengths by adiabatically ramping the total RF voltage during the initial 15 ms to values between the initial 25 kV and 80 kV. Due to varying shot-to-shot efficiency of the C16 blow-up, we achieve total bunch lengths over a range of $B_L = 130 \,..\, 220$ ns. Figure 7a depicts consistently depressed peak line densities by a factor 0.9 for the flattened

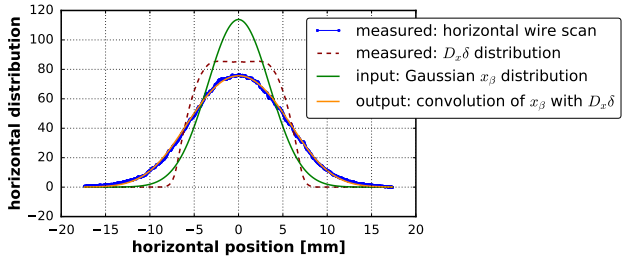

Figure 6: Wire scan comprising betatron and dispersive part.

profiles compared to the parabolic ones. A theoretically ideal rectangular profile of $4\sigma_z$ length would yield a $\sqrt{2\pi}/4 \approx 0.63$ depression factor compared to a perfect Gaussian. Both extrema are plotted in Fig. 7a for comparison.

We want to compare the impact of space charge for both beam types for fixed B_L, N and ϵ_u. To unify this set in one quantity, we choose to evaluate $\Delta Q_u^{\max}$ assuming a 6D Gaussian distributed beam in Eq. (1). Hence we apply (2) as well as using the Gaussian peak line density $\lambda_{\max} = N/(\sqrt{2\pi}\sigma_z)$ where we set $\sigma_z = B_L/4$. Figure 7b shows how hollow bunches provide statistically significantly lower vertical emittances for the same unified reference tune shift $\Delta Q_u^{\max}$. The real tune shift of the hollow bunches is a factor 0.88 lower due to their reduced $\lambda_{\max}$ and the larger σ_x. In contrast, the parabolic bunches are rather well represented by the Gaussian approach (factor 0.97 lower real tune shift).

Finally, keeping the maximum RF voltage 80 kV, we scan the intensity by varying the injected turns in the PSB. Figure 7c exhibits the emittance blow-up $\epsilon_y^{\mathrm{fin}}/\epsilon_y^{\mathrm{ini}}$ versus the brightness, which is again lower for the hollow bunches.

CONCLUSION

We have set up a reliable process to create hollow bunches with minimal changes to the operational PSB cycle. Due to the lower peak line density, the hollow bunches are shown to be less affected by space charge compared to the parabolic bunches during the PS injection plateau.

ACKNOWLEDGEMENT

The PSB feedback systems have been set up to create and transfer hollow bunches owing to the invaluable support by Maria-Elena Angoletta and Michael Jaussi.

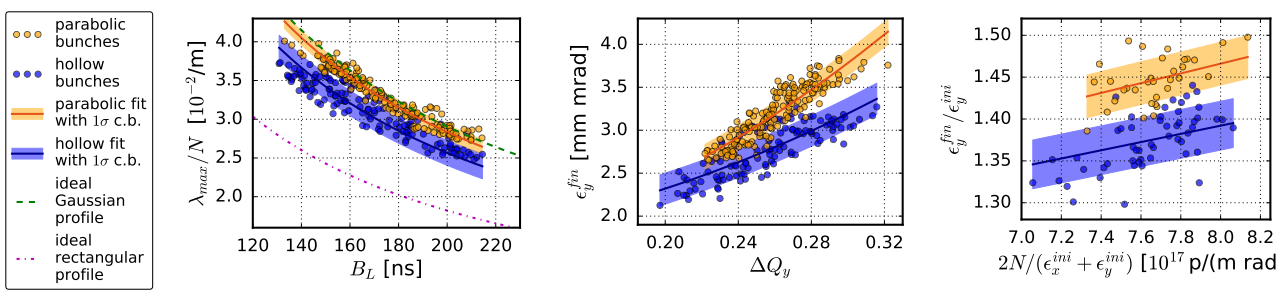

(a) Intensity normalised peak line charge density vs. total bunch length.

(b) Vertical emittances (end of inject. plateau) vs. space charge tune shift.

(c) Vertical emittance blow-up vs. brightness (at $V_{\mathrm{rf}} = 80$ kV).

Figure 7: Comparison of hollow and parabolic bunches. Fits include 1σ confidence bands [5].

ISBN 978-3-95450-178-6

REFERENCES

[1] H. Damerau *et al.*, "LHC Injectors Upgrade, Technical Design Report, Vol. I: Protons", CERN-ACC-2014-0337, Geneva, Switzerland, 2014.

[2] H. Bartosik *et al.*, "Can We Ever Reach the HL-LHC Requirements with the Injectors?", in *RLIUP: Review of LHC and Injector Upgrade Plans*, Archamps, France, Oct. 2013, pp. 95-104.

[3] R. Wasef *et al.*, "Space Charge Effects and Limitations in the CERN Proton Synchrotron", in *Proc. 4th Int. Particle Accelerator Conf. (IPAC'13)*, Shanghai, China, May 2013, paper WEPEA070, pp. 2669-2671.

[4] S. Gilardoni *et al.*, "LIU: Which Beams in the Injectors Fulfill HL-LHC Upgrade Scenario 1 Goals?", in *RLIUP: Review of LHC and Injector Upgrade Plans*, Archamps, France, Oct. 2013, pp. 69-73.

[5] A. Oeftiger, H. Bartosik, A. Findlay, S. Hancock and G. Rumolo, "Flat Bunches With a Hollow Distribution for Space Charge Mitigation", in *Proc. 7th Int. Particle Accelerator Conf. (IPAC'16)*, Busan, Korea, May 2016, paper MOPOR023, pp. 652-655.

[6] R. Cappi, R. Garoby, S. Hancock, M. Martini, J.P. Riunaud, "Measurement and Reduction of Transverse Emittance Blow-up Induced by Space Charge Effects", in *Proc. 15th IEEE Particle Accelerator Conf. (PAC'93)*, Washington, DC, USA, May 1993, pp. 3570-3572.

[7] R. Garoby and S. Hancock, "New Techniques for Tailoring Longitudinal Density in a Proton Synchrotron", in *Proc. 4th European Particle Accelerator Conf. (EPAC'94)*, London, UK, June 1994, pp. 282.

[8] K. Schindl, "Space Charge", CERN/PS 99-012(DI), Geneva, Switzerland, 1999.

[9] R. Baartman, "Betatron Resonances With Space Charge", in *AIP Conference Proceedings*, vol. 448, 1998, pp. 56-72.

[10] H. Huang *et al.*, "Experimental Determination of the Hamiltonian for Synchrotron Motion with RF Phase Modulation", in *Phys. Rev. E*, vol. 48, no. 6, Dec. 1993, pp. 4678-4688.

[11] S. Hancock, S.R. Koscielniak, M. Lindroos, "Longitudinal Phase Space Tomography with Space Charge", in *Proc. 7th European Particle Accelerator Conf. (EPAC 2000)*, Vienna, Austria, Jul. 2000, pp. 1726-1728.

[12] S.Y. Lee, "Accelerator Physics", World Scientific, 3rd edition, 2012.

[13] A.W. Chao, "Physics of Collective Beam Instabilities in High Energy Accelerators", Wiley, 1993.

[14] M. Reiser, "Theory and Design of Charged Particle Beams", John Wiley & Sons, Jun. 2008.

[15] E. Metral *et al.*, "Beam Instabilities in Hadron Synchrotrons", in *IEEE Transactions on Nuclear Science*, vol. 63, no. 2, Apr. 2016, pp. 1001-1050.

[16] K.S.B. Li *et al.*, "Code development for Collective Effects", presented at the ICFA Advanced Beam Dynamics Workshop on High-Intensity and High-Brightness Hadron Beams (HB2016), Malmö, Sweden, July 2016, paper WEAM3X01, this conference.

[17] A. Oeftiger and S. Hegglin, "Space Charge Modules for PyHEADTAIL", presented at the ICFA Advanced Beam Dynamics Workshop on High-Intensity and High-Brightness Hadron Beams (HB2016), Malmö, Sweden, July 2016, paper MOPR025, this conference.

[18] A. Oeftiger, "Space Charge Effects and Advanced Modelling for CERN Low Energy Machines", unpublished Ph.D. thesis, LPAP, EDPY, École Polytechnique Fédérale de Lausanne, Lausanne, Switzerland, 2016.

[19] G. Rumolo, O. Boine-Frankenheim, I. Hofmann, Y. Liu and A. Al-Khateeb, "Effects of Space Charge on Decoherence in Ion Beams", in *Proc. Particle Accelerator Conf. (PAC 2003)*, Portland, USA, May 2003, vol. 4, pp. 2607-2609.

[20] A. Oeftiger, H. Bartosik, A.J. Findlay, S. Hancock and G. Rumolo, "MD210 Note: Creation of Hollow Bunches in the PSB", CERN-ACC-NOTE-2016-0045, Geneva, Switzerland, Jun. 2016.

ISBN 978-3-95450-178-6